Damping of Growth Oscillations in Molecular Beam Epitaxy: A Renormalization Group Approach

Martin Rost*and Joachim Krug
Fachbereich Physik
Universität GH Essen
D-45117 Essen, Germany

February 1, 2008

Abstract

The conserved Sine–Gordon Equation with nonconserved shot noise is used to model homoepitaxial crystal growth. With increasing coverage the renormalized pinning potential changes from strong to weak. This is interpreted as a transition from layer–by–layer to rough growth. The associated length and time scales are identified, and found to agree with recent scaling arguments. A heuristically postulated nonlinear term $\nabla^2(\nabla h)^2$ is created under renormalization.

1 Introduction

In Molecular Beam Epitaxy (MBE) it is possible to control the amount of deposited matter through oscillations of the surface roughness, which indicate that the surface grows layer by layer [1, 2, 3]. A simple picture represents layer-by-layer growth on a high symmetry surface as follows: After deposition out of the beam atoms diffuse on the surface until they either meet other diffusing atoms to form a stable island, or get incorporated at the edge of a previously nucleated island. If most atoms deposited on top of an island are assumed to be incorporated into its edge by performing a downward hop (which implies that the suppression of interlayer transport by Ehrlich-Schwoebel-barriers [4] is negligible), little nucleation occurs in the second crystal layer before the first layer is completed.

*Email: marost@theo-phys.uni-essen.de. Fax: 49-201-183 2120.

Consequently the surface width at layer completion is nearly zero, after having gone through a maximum at half filling of the first layer. As long as the layer-by-layer growth mode persists, the surface morphology exhibits oscillations with a period given by the monolayer completion time.

In general this scenario is only transient, and the oscillations are damped. A variety of mechanisms contribute to the damping: The surface may be slightly miscut [2, 5], or the average beam intensity may be inhomogeneous [3]. However, even in the absence of such (experimentally unavoidable) imperfections, the stochastic beam fluctuations are sufficient to destroy the temporal coherence of spatially separated regions on the surface. Provided the beam noise is the sole damping mechanism, it was recently shown that the critical coverage $\tilde{\theta}$ at which the oscillations disappear scales with the ratio of the surface diffusion constant D_S to the deposition flux F as [6, 7]

$$\tilde{\theta} \sim (D_S/F)^{\delta} \tag{1}$$

with an exponent

$$\delta = \gamma \frac{4d}{4-d}, \tag{2}$$

where d denotes the surface dimensionality ($d = 2$ for real surfaces) and the exponent γ characterizes the dependence of the diffusion length (or typical island size) ℓ_D on D_S/F [8],

$$\ell_D \sim (D_S/F)^{\gamma}. \tag{3}$$

Eq.(1) may therefore be rewritten as

$$\tilde{\theta} \sim \ell_D^{4d/(4-d)} \sim \tilde{\ell}^d \tag{4}$$

where

$$\tilde{\ell} \sim \ell_D^{4/(4-d)} \tag{5}$$

is the coherence length, an estimate of the size of coherently oscillating regions [7].

The theory of Ref.[7] is based on a phenomenological stochastic continuum equation for the growing surface. It is not clear *a priori* that such a continuum description would be able to capture the phenomenon of growth oscillations, which is distinctly a lattice effect. As a first step towards a more complete treatment, in the present work we therefore *perturbatively* include the lattice structure by analyzing the driven, conserved sine-Gordon equation

$$\partial_t h = -K\Delta^2 h - \lambda\Delta(\nabla h)^2 - V\Delta \sin\frac{2\pi h}{a_\perp} + F + \eta \tag{6}$$

for the surface height $h(\mathbf{x}, t)$. In this equation the constant F denotes the average deposition flux, while the noise $\eta(\mathbf{x}, t)$ models its "shot noise" fluctuations. The noise is assumed to be Gaussian with mean zero and correlator

$$\langle \eta(\mathbf{x}, t)\eta(\mathbf{x}', t')\rangle = 2D\ \delta(t - t')\delta(\mathbf{x} - \mathbf{x}'). \tag{7}$$

To motivate the systematic terms on the right hand side of eq.(6), we note that it can be written in the form of a continuity equation

$$\partial_t h + \nabla \cdot \mathbf{J} = F + \eta \tag{8}$$

reflecting the absence of desorption and defect formation under typical MBE conditions [9, 10, 11]. The current is given by Fick's law, $\mathbf{J} = -\nabla\rho$, where the quantity

$$\rho(\mathbf{x}, t) = -K\Delta h - \lambda(\nabla h)^2 - V \sin \frac{2\pi h}{a_\perp} \tag{9}$$

can be interpreted as the spatially varying part of a coarse grained adatom density [9] or chemical potential [11]. The first term incorporates a generalized Gibbs-Thomson effect [12], according to which the density is enhanced near maxima and decreased near minima of the surface, while the second term reflects the dependence of the density on the local vicinality [7, 11, 13]. The third term models the lattice potential: Adatoms are preferably driven to places where they can be incorporated such that the surface remains at integer multiples of the vertical lattice constant $a_\perp$. Only the lowest harmonic of the periodic surface potential is kept, since components of periodicity $a_\perp/2, a_\perp/3, \ldots$ are less relevant (see below and [14]). It is necessary to distinguish the vertical ($a_\perp$) and horizontal ($a_\parallel$) lattice constants, since they play very different roles in the renormalization group calculation.

The analysis of Ref.[7] was based on eq.(6) with $V = 0$. Here we show that, by explicitly including the lattice potential, the characteristic time and length scales (1,5) emerge naturally in the renormalization group (RG) flow equation of the potential strength V. Moreover the $(\nabla h)^2$ nonlinearity in (9) is seen to be generated under renormalization, thus relieving us from the task of postulating its microscopic origin; we may set $\lambda = 0$ microscopically. A similar scenario is valid for the nonconserved Sine–Gordon model [15]. These results are obtained by applying the Nozières-Gallet RG scheme [14] to eq.(6). An RG analysis of (6) was previously presented by Tang and Nattermann [16], however these authors considered separately the cases $V = 0$, $\lambda \neq 0$ and $V \neq 0$, $\lambda = 0$ and thus were not able to address the generation of λ from the lattice potential; in addition, our analysis includes explicitly the flat initial condition of the surface, which is essential for describing transient behavior.

Since the interpretation of the RG results depends crucially on relating the "mesoscopic" coefficient K to the microscopic length scale ℓ_D, the next section will address this issue within the framework of the linear equation ($V = \lambda = 0$). It turns out that the mere existence of a vertical lattice constant $a_\perp$ is sufficient for the nontrivial time and length scales (1,5) to emerge from the continuum theory, even if this scale has no dynamical effect (i.e., $V = 0$) [17]. The full problem with $V \neq 0$ is treated in the following sections. After briefly recalling the RG scheme, the renormalization of the conserved Sine–Gordon Equation in 2+1 dimensions

is carried out in Section 3. The RG–flow equations for the parameters in Eq. (6) are interpreted in Section 4, and the extension to general dimensionalities and general relaxation mechanisms is briefly addressed. Some conclusions are given in Section 5.

2 Length scales in the linear theory

On the most basic level, the growing surface morphology evolves in response to the competition between disordering beam fluctuations and smoothening surface diffusion. The simplest continuum theory that incorporates both effects is the linearization of (6),

$$\partial_t h = -K\Delta^2 h + F + \eta. \tag{10}$$

As was mentioned in Section 1, the coefficient K arises from an expansion of the local adatom density in the surface curvature Δh. Under near-equilibrium conditions, it would therefore be expected to be given by the product of the surface stiffness and the adatom mobility [12, 18]. However, far from equilibrium other processes may contribute to, and in fact dominate K [9, 19]. In particular, it has been suggested [20] that random island nucleation produces a contribution

$$K \sim F\ell_D^4, \tag{11}$$

but the underlying microscopic mechanism is not known. In the following we show how this relation follows from a simple reinterpretation of (10) in the presence of a finite vertical lattice constant $a_\perp$.

The straightforward solution of (10) [11] shows that, starting from a flat substrate at time $t = 0$, after time t surface correlations have developed up to a scale

$$\xi(t) \approx (Kt)^{1/4} \tag{12}$$

and the surface width grows as

$$W(t) \approx (D/K)^{1/2}\xi(t)^\zeta \tag{13}$$

in dimensionalities $d < 4$, where

$$\zeta = \frac{4-d}{2} \tag{14}$$

is the roughness exponent of the linear equation [11].

Together with the average growth rate F the presence of the vertical lattice constant induces a fundamental time scale, the monolayer completion time

$$\tau_{\mathrm{ML}} = a_\perp/F. \tag{15}$$

Setting $t = \tau_{\mathrm{ML}}$ in (12) we obtain a corresponding lateral length scale $\xi(\tau_{\mathrm{ML}})$, the scale on which lateral structure has developed after deposition of one monolayer. Clearly it is very natural to identify this scale with the diffusion length ℓ_D, and hence the coefficient K in (12) can be identified as

$$K \approx \ell_D^4/\tau_{\mathrm{ML}} = a_\perp^{-1} F \ell_D^4 \tag{16}$$

in accordance with (11). The correlation length (12) can then be expressed in terms of the coverage $\theta = Ft/a_\perp$ as

$$\xi(t) \approx \ell_D \theta^{1/4}. \tag{17}$$

To see how the scaling laws (1) and (5) can be obtained along similar lines, note first that for shot noise the noise strength D is proportional to the beam intensity F,

$$D \approx a_\perp a_\parallel^d F. \tag{18}$$

Thus (13) takes the form

$$W \approx a_\perp (a_\parallel/\ell_D)^{d/2} \theta^{(4-d)/8}. \tag{19}$$

If one now postulates, plausibly [7], that the lattice effects disappear when the roughness due to long wavelength fluctuations becomes comparable to $a_\perp$, the characteristic coverage $\tilde{\theta}$ can be defined through $W(\tilde{\theta}) \approx a_\perp$ and is given precisely by eqs. (1) and (2).

These considerations may be viewed as a zeroth order assessment of lattice effects, to be justified by the systematic calculation provided in the remainder of the paper. They easily extended to general linear equations with a dynamical exponent z [11], in which case one finds [7]

$$\delta = \gamma \frac{zd}{z-d} \tag{20}$$

for $z > d$.

3 Renormalization Group Analysis

3.1 The Renormalization Scheme of Nozières and Gallet

Because of the structure of Equation (6) we use an approach which is suitable for general forms of the nonlinearity. It was introduced by Nozières and Gallet for the dynamical renormalization of the Sine-Gordon equation to obtain the roughening transition [14]. A detailed presentation can be found in their work, which we recall briefly.

Consider a Langevin equation

$$\partial_t h = \mathcal{L}h + \mathcal{N}(h) + \eta \tag{21}$$

with a linear part $\mathcal{L}h$, a nonlinear term $\mathcal{N}(h)$ and Gaussian noise η with mean zero and correlator $\langle \eta(\mathbf{k},t)\eta(\mathbf{k}',t')\rangle = 2|\mathbf{k}|^{2\mu} D\delta(t-t')\delta(\mathbf{k}+\mathbf{k}')\theta(|\mathbf{k}|-\Lambda)$. The cutoff $\Lambda \equiv 1/a_\parallel$ is introduced to model the lateral lattice structure which does not allow for fluctuations on scales smaller than the horizontal lattice constant $a_\parallel$. In the following $a_\parallel$ will only appear in the cutoff Λ, hence we can disregard the distinction between $a_\parallel$ and $a_\perp$ and set $a_\perp = a$.

Two types of noise can be considered: Either volume conserving noise, which corresponds to the case $\mu = 1$ ("diffusion noise" [6]), or nonconserving "shot" noise $\mu = 0$. Here we focus on the nonconserved contribution, $\mu = 0$, which always dominates on scales larger than the diffusion length ℓ_D [7, 6]. A study of the conserved case has been presented in Ref.[21].

Renormalization of Equation (21) is performed in the following way:

- We average over the short wave components $\delta\eta$ of the noise. In $\mathbf{k}$–space $\delta\eta$ is nonzero only for modes $\mathbf{k}$ with $(1-dl)\Lambda < |\mathbf{k}| \leq \Lambda$. Define the averaged or coarse grained field $\bar{h} \equiv \langle h \rangle_{\delta\eta}$.

- Equation (21) is split in two; one for the coarse grained field

  $$\partial_t \bar{h} = \mathcal{L}\bar{h} + \langle \mathcal{N}(\bar{h} + \delta h)\rangle_{\delta\eta} + \bar{\eta}$$

  and a second one for the difference $\delta h \equiv h - \bar{h}$. One now takes an approximation of $\langle \mathcal{N}(\bar{h}+\delta h)\rangle_{\delta\eta}$ in terms of the (hopefully all) relevant operators appearing in Equation (21). For this one calculates δh (respectively its correlation functions) perturbatively in the nonlinearity $\mathcal{N}$. Since $\mathcal{N}$ is not of a simple polynomial form, a Rayleigh–Schrödinger expansion is used – the only one feasible one, albeit poorly controlled.

- Time, lateral and vertical length are rescaled with different exponents: $\mathbf{x} \to (1-dl)\mathbf{x}$, $h \to (1-\zeta\, dl)h$ and $t \to (1-z\, dl)t$. This causes a corresponding rescaling of the terms in (21) yielding the RG flow equations for $\mathcal{L}$ and $\mathcal{N}$.

The detailed application of these steps to Equation (6) is the subject of the next section.

3.2 Application to the Conserved Sine–Gordon Equation

Consider Equation (6) in a frame moving with the average growth speed F

$$\partial_t h = -K\Delta^2 h - V\ \Delta \sin\frac{2\pi}{a}\Big(h - Ft\Big) + \eta. \tag{22}$$

Epitaxial growth starts on an atomically flat surface, so at time $t=0$ the initial configuration is $h\equiv 0$. Fluctuations are caused by the noise at *later* times. This will play an important role in the interpretation of our results.

We neglect the perturbative contribution of the $-\lambda\Delta(\nabla h)^2$–term. As argued in the Introduction on a microsopic level it is absent. It is generated by the lattice potential and the driving force F to order V^2. Although it is a relevant operator at the linear fixed point, we expect it to be negligible on small and intermediate scales, as long as the lattice potential contributes to renormalization of K and λ. The same is observed for the $(\nabla h)^2$–nonlinearity in the nonconserved Sine–Gordon Equation [15].

Averaging over $\delta\eta$ leads to two coupled equations, where we expand to lowest order in the infinitesimal quantity δh

$$\begin{aligned}
\partial_t \bar{h} &= -K\,\Delta^2\bar{h} - V\Delta\left[\sin\frac{2\pi}{a}\Big(\bar{h}-Ft\Big)\left(1-\frac{2\pi^2}{a^2}\langle\delta h^2\rangle\right)\right] + \bar{\eta} \\
\partial_t \delta h &= -K\,\Delta^2\delta h - V\Delta\left[\cos\frac{2\pi}{a}\Big(\bar{h}-Ft\Big)\;\frac{2\pi}{a}\;\delta h\right] + \delta\eta.
\end{aligned} \tag{23}$$

The second equation of (23) is solved by a Rayleigh–Schrödinger perturbation ansatz

$$\begin{aligned}
\delta h^{(0)}(\mathbf{x},t) &= \int d^dx' \int_0^t dt'\; G(\mathbf{x}-\mathbf{x}',t-t')\;\delta\eta(\mathbf{x}',t') \\
\delta h^{(1)}(\mathbf{x},t) &= -\frac{2\pi V}{a}\int d^dx' \int_0^t dt'\; G(\mathbf{x}-\mathbf{x}',t-t')\;\times \\
&\qquad \Delta'\left[\cos\frac{2\pi}{a}\Big(\bar{h}(\mathbf{x}',t')-Ft'\Big)\;\delta h^{(0)}(\mathbf{x}',t')\right].
\end{aligned} \tag{24}$$

In $\mathbf{k}$–space the linear propagator G is given by $\exp -K(t-t')|\mathbf{k}|^4$. In the sequel we will use the notation $\bar{h}', \eta', \ldots$ when the argument is the integration variable $(\mathbf{x}',t')$ and unprimed symbols for quantities at $(\mathbf{x},t)$. The corresponding derivatives (Laplace operators) are denoted Δ and Δ' to mark this difference. For the convolution integral $\int d^dx' \int_0^t dt'$ the shorthand $\int$ is used.

Insertion of $\langle\delta h^2\rangle = \langle{\delta h^{(0)}}^2\rangle + 2\langle\delta h^{(0)}\delta h^{(1)}\rangle + O(V^2)$ in the first equation of (23) generates the corrective terms for $\bar{h}$ to order V^2.

$$\langle\delta h^2\rangle = \langle{\delta h^{(0)}}^2\rangle - \frac{4\pi V}{a}\int(\Delta' G)\;\cos\frac{2\pi}{a}\Big(\bar{h}'-Ft'\Big)\;C, \tag{25}$$

where $C \equiv \langle\delta h^{(0)}\delta h^{(0)\prime}\rangle$ is the unperturbed correlator. Its Fourier transform is given by $e^{-K(t-t')|\mathbf{k}|^4} D/(K|\mathbf{k}|^4)\left[1-e^{-2Kt|\mathbf{k}|^4}\right]$.

The lowest order term $\langle{\delta h^{(0)}}^2\rangle$ is a constant which multiplies the sine potential, yielding the correction

$$\delta V = -\frac{4\pi^3 D}{Ka^2\Lambda^2}\left(1-e^{-2K\Lambda^4 t}\right)\;dl\;V. \tag{26}$$

In general dimension $2\pi/\Lambda^2$ is replaced by $S_d\Lambda^{d-4}$, where S_d is the surface area of the d-dimensional unit sphere.

To handle the next order contribution due to $\langle\delta h^{(0)}\delta h^{(1)}\rangle$,

$$-\frac{8\pi^3V^2}{a^3}\ \Delta\int\sin\frac{2\pi}{a}\Big(\bar h-Ft\Big)\ \cos\frac{2\pi}{a}\Big(\bar h'-Ft'\Big)\ (\Delta' G)\ C,$$

we split the product $\sin\alpha\cos\beta = (\sin(\alpha+\beta)+\sin(\alpha-\beta))/2$ and discard the term with $\sin(\alpha+\beta)$. It would create higher harmonics of the lattice potential, which are less relevant (see Eq. (26)) than the fundamental. In the remaining expression we split into terms with $\bar h$ and Ft

$$\begin{aligned}-\frac{4\pi^3V^2}{a^3}\ \ \Delta\ \ \int\Bigg[&\sin\frac{2\pi}{a}F(t'-t)\ \cos\frac{2\pi}{a}\Big(\bar h-\bar h'\Big)\ (\Delta' G)\ C\\ &+\ \ \cos\frac{2\pi}{a}F(t'-t)\ \sin\frac{2\pi}{a}\Big(\bar h-\bar h'\Big)\ (\Delta' G)\ C\Bigg].\end{aligned}$$

Expanding terms with $\bar h-\bar h'$ in powers of $\xi\equiv\mathbf{x}'-\mathbf{x}$ and taking care of the symmetries when integrating over $d^2\xi$ we get

$$\begin{aligned}=\qquad&\frac{4\pi^5V^2}{a^5}\Big[\Delta(\nabla\bar h)^2\Big]\ \int\sin\Big[\frac{2\pi}{a}F(t'-t)\Big]\ (\Delta' G)\ C\ \xi^2\\ -\ \ &\frac{2\pi^4V^2}{a^4}\Big[\Delta^2\bar h\Big]\ \int\cos\Big[\frac{2\pi}{a}F(t'-t)\Big]\ (\Delta' G)\ C\ \xi^2.\end{aligned}\tag{27}$$

Up to now we have expanded the averaged nonlinearity $\langle\mathcal{N}(h)\rangle_{\delta\eta}$ to order V^2 in projections onto the relevant operators.

The last step consists in rescaling space and time. To examine the behavior close to the linear fixed point $V=0,\lambda=0$ we choose its scaling exponents, $z=4$ and $\zeta=2-d/2=1$ in two dimensions (see (14)). Accordingly the growth rate F and the lattice constants $a_\perp$ and $a_\parallel$ are rescaled as $dF/dl=(z-\zeta)F$, $da_\perp/dl=-\zeta a_\perp$ and $da_\parallel/dl=-a_\parallel$.

3.3 Flow equations

The RG flow will be examined in terms of dimensionless quantities, in which the effect of the trivial rescaling has been eliminated. As elementary length scales we use the vertical and horizontal lattice constants $a_\perp$ and $a_\parallel$, and the basic time scale is given by the monolayer completion time $\tau_{\rm ML}=a_\perp/F$. Thus time is measured through the coverage $\theta=t/\tau_{\rm ML}$, and the coefficients K, V and λ appearing in (6) are replaced by the expressions

$$\mathcal{K}\equiv\frac{Ka_\perp}{Fa_\parallel^4}=(\ell_D/a_\parallel)^4$$

$$U = \frac{V}{F a_\parallel^2}$$

$$L = \frac{\lambda a_\perp^2}{F a_\parallel^4}.$$

Due to the conserved form of the equation of motion (6), the noise strength D is not renormalized [10, 16], and need not be considered further.

Using the scaling parameter $\kappa \equiv \exp 4l$, the flow equations then take the form

$$\begin{aligned}
\text{(i)} \quad & 4\kappa \frac{dU}{d\kappa} &=& -4\pi^3 \frac{\sqrt{\kappa}}{\mathcal{K}} \left(1 - e^{-2\mathcal{K}\theta/\kappa}\right) U, \\
\text{(ii)} \quad & 4\kappa \frac{d\mathcal{K}}{d\kappa} &=& \frac{\sqrt{\kappa}\, U^2}{\mathcal{K}}\ g(\mathcal{K}/\kappa, \theta), \\
\text{(iii)} \quad & 4\kappa \frac{dL}{d\kappa} &=& \frac{\sqrt{\kappa}\, U^2}{\mathcal{K}}\ f(\mathcal{K}/\kappa, \theta).
\end{aligned} \tag{28}$$

The functions f and g depend on the integrals in Eq. (27) and are given in the appendix. Equations (28) are the central result of this paper. The following sections are devoted to the discussion of their physical content.

4 Interpretation of the RG Results

As in the case of the roughening transition [14], the renormalization of U determines the relevance of the lattice on large scales. In the present situation the lattice potential always decreases under renormalization (eq.(28(i))). Indeed, since in the absence of the lattice potential the roughness exponent (14) $\zeta > 0$ in two dimensions, the lattice becomes irrelevant asymptotically; a roughening transition is possible only if $\zeta = 0$, such as for eq.(6) subject to conserved noise [21]. Nevertheless on finite length or time scales U remains finite, and its dependence on θ and κ may be used to describe the transition from (lattice-dominated) layer-by-layer growth to rough, continuous growth. It can be shown that for small U the amplitude of the surface width oscillations is proportional to U; thus the value of U on a given time or length scale is a direct measure of the observable signatures of layer-by-layer growth.

In the following we assume that the rate of particle deposition is small compared to the diffusion rate, which is true for typical MBE conditions and implies that the dimensionless stiffness parameter $\mathcal{K} \gg 1$. The renormalization of $\mathcal{K}$ due to the lattice potential, as expressed by eq.(28(ii)), can then be disregarded, and $\mathcal{K}$ becomes a constant. This decouples the flow equation for the lattice potential U and allows for a straightforward solution, which can be used to extract the damping time $\tilde{\theta}$ and the coherence length $\tilde{\ell}$. In Section 4.3 the generation of the $\Delta(\nabla h)^2$ nonlinearity, as described by eq.(28(iii)), will be discussed.

4.1 Damping time

The asymptotic ($\kappa \to \infty$) value of the lattice potential U is obtained from eq.(28(i)) as

$$U_\infty = e^{-I(\theta)} U_0 \tag{29}$$

with

$$I(\theta) = \frac{\pi^3}{\mathcal{K}} \int_1^\infty \frac{d\kappa}{\sqrt{\kappa}} (1 - e^{-2\mathcal{K}\theta/\kappa}) \approx \sqrt{8\pi^7 \theta/\mathcal{K}} \tag{30}$$

in the relevant regime $\mathcal{K}\theta \gg 1$. Thus writing $I(\theta) = \sqrt{\theta/\tilde{\theta}}$ the characteristic coverage is obtained as

$$\tilde{\theta} = \frac{\mathcal{K}}{8\pi^7} \sim (\ell_D/a_\parallel)^4, \tag{31}$$

in agreement with (4) for $d = 2$. Moreover, since in this case the surface width of the linear theory is proportional to $(\theta/\tilde{\theta})^{1/4}$ (see Section 2), we see that the decay of the lattice potential is of the form

$$U_\infty/U_0 \approx \exp[-CW^2(\theta)] \tag{32}$$

where $C > 0$ is a constant. This behavior has been found to describe the decay of oscillation amplitudes in layer-by-layer growth in numerical simulations, and can be derived assuming a discrete probability distribution of the heights taking at each possible height the value of the corresponding continuous Gaussian distribution [22].

It is instructive to extend these results to other dimensionalities and linear relaxation mechanisms with a general dynamic exponent z. For general z, the natural scaling variable is $\kappa = \exp zl$. Then the only qualitative change of the expressions discussed above is that the algebraic part of the integrand in (30) becomes $\kappa^{2\zeta/z-1}$ instead of $\kappa^{-1/2}$. To see this, note that the only quantity changing under rescaling in the time-independent part of the correction $\delta V/V$ in eq.(26) is the vertical lattice spacing $a_\perp \sim \kappa^{-\zeta/z}$. Thus, for $\zeta < 0$ the integral (30) converges even when $\theta \to \infty$, implying that the surface remains smooth. For $\zeta > 0$ the integral becomes

$$I(\theta) \sim \mathcal{K}^{-1} (\mathcal{K}\theta)^{2\zeta/z} \sim W^2, \tag{33}$$

showing that (32) remains valid in the general case. Writing $I(\theta) = (\theta/\tilde{\theta})^{2\zeta/z}$, the characteristic coverage is of the order

$$\tilde{\theta} \sim \mathcal{K}^{z/2\zeta-1} = \mathcal{K}^{d/(z-d)}, \tag{34}$$

where in the last step the scaling relation $z = d + 2\zeta$ for linear growth equations [11] has been used. This becomes equivalent to (20) by noting that (16) is replaced by $K \approx \ell_D^z/\tau_{\mathrm{ML}}$ for general z.

4.2 Coherence length

For $\theta \to \infty$ the solution of the flow equation (28(i)) at finite κ is

$$U(\kappa) = \exp[-(2\pi^3/\mathcal{K})(\sqrt{\kappa} - 1)]U_0. \tag{35}$$

If the renormalization is stopped at a lateral scale $L_\parallel = \kappa^{1/4} a_\parallel$, the remaining value of the lattice potential may therefore be written, for $L_\parallel/a_\parallel \gg 1$, as

$$U(L_\parallel)/U_0 = e^{-(L_\parallel/\tilde{\ell})^2} \tag{36}$$

with

$$\tilde{\ell} = a_\parallel \sqrt{\frac{\mathcal{K}}{2\pi^3}} \sim \frac{\ell_D^2}{a_\parallel}, \tag{37}$$

in agreement with the expression (5) for the coherence length. If the system is smaller than $\tilde{\ell}$ the lattice potential remains relevant, the surface remains smooth and growth oscillations will be present for all times [7].

As in the previous section, these considerations can be generalized to arbitrary z and d. Then (36) becomes $U(L_\parallel)/U_0 = \exp[-(L_\parallel/\tilde{\ell})^{2\zeta}]$ with

$$\tilde{\ell} \sim \mathcal{K}^{1/2\zeta} = \mathcal{K}^{1/(z-d)} \sim (\ell_D/a_\parallel)^{z/(z-d)} \tag{38}$$

in accordance with (20) and Ref.[7].

4.3 Generation of the conserved KPZ nonlinearity

We now focus on the flow equation (28(iii)), which describes the generation of the nonlinear term of the conserved Kardar-Parisi-Zhang [23] (CKPZ) equation, $\Delta(\nabla h)^2$, through the interplay of the lattice potential V, the growth rate F and the effective stiffness K. We consider the stationary regime $\theta \to \infty$, and again assume that $\mathcal{K}$ is large, so that its renormalization can be neglected. Setting $L = \lambda = 0$ at the microscopic scale, the solution of the flow equation (28(iii)) then reads

$$L(\kappa) = \frac{U_0^2}{4\mathcal{K}} \int_1^\kappa dx\; x^{-1/2}\; \exp[-(4\pi^3/\mathcal{K})(\sqrt{x} - 1)] f(\mathcal{K}/x), \tag{39}$$

where the solution (35) for the flow of U has been used. For $\kappa \to \infty$, eq.(39) tends to a finite limit, which for $\mathcal{K} \to \infty$ has the simple form

$$L_\infty = 2\pi^2 U_0^2. \tag{40}$$

The numerical solution of the full set (28) of coupled flow equations shows that the limiting value (40) is attained for $\mathcal{K} \geq 10^8$, corresponding to a diffusion length

$\ell_D = 100 a_\parallel$. In the range $10^4 \leq \mathcal{K} \leq 10^8$ the nonlinear coupling $L\infty$ is positive and increases with increasing $\mathcal{K}$, while for smaller values of $\mathcal{K}$ it is negative.

In terms of the bare parameters of the original equation, the relation (40) implies that, on large scales and for large diffusion lengths, the CKPZ coefficient λ is positive and of the form

$$\lambda \approx \frac{V_0^2}{F a_\perp^2}. \tag{41}$$

It is instructive to compare this to a heuristic estimate of λ, based on Burton-Cabrera-Frank (BCF) theory [7, 11]. According to BCF [24], the adatom density on a terrace can be computed by solving a steady state diffusion equation with sinks at the surface steps. The density decreases with decreasing step distance or increasing tilt, and becomes independent of the tilt when the step distance is of the order of the diffusion length ℓ_D. The coefficient λ of the leading order expansion (9) around a singular surface is then positive[1] and given by

$$\lambda_{\mathrm{BCF}} \approx \frac{F \ell_D^4}{a_\perp^2}. \tag{42}$$

To identify eqs.(41) and (42) we would need to require that the bare pinning potential V_0 depends on the diffusion length as $V_0 \approx F \ell_D^2$, and hence the dimensionless potential strength is

$$U_0 \approx (\ell_D / a_\parallel)^2 = \sqrt{\mathcal{K}} \gg 1, \tag{43}$$

which is clearly inconsistent with our perturbative treatment of the potential. Thus, the expressions (41) and (42) are *not* equivalent, but rather correspond to different limiting situations: Our calculation is an expansion for small U_0 and fixed (large) $\mathcal{K}$, while the BCF picture assumes perfect crystal planes, which would be formally represented by taking $U_0 \to \infty$ at fixed $\mathcal{K}$. Writing $L_\infty = L_\infty(U_0, \mathcal{K})$ we have shown that $L_\infty = U_0^2 \ \phi(\mathcal{K})$ for $U_0 \to 0$, where ϕ is an increasing function of $\mathcal{K}$, and the BCF argument indicates that $L_\infty \sim \mathcal{K}$ for $U_0 \to \infty$. Clearly the latter regime is not accessible by our method. Nevertheless it is remarkable that the CKPZ coefficient emerges from the RG calculation with the correct sign and the correct qualitative dependence on the diffusion length.

5 Conclusions

In this work we have derived renormalization group flow equations for the conserved Sine–Gordon Equation with nonconserved shot noise. They were used to model the crossover in homoepitaxy from layer–by–layer growth to rough growth.

[1] For a vicinal surface growing in the step flow mode one can show that $\lambda < 0$, see [13].

The crossover can be quantitatively characterized by a characteristic *layer coherence length* $\tilde{\ell}$ and an associated coverage $\tilde{\theta}$, which is a measure of the number of growth oscillations that can be observed under optimal growth conditions (that is, in the absence of miscut or beam inhomogeneity). The dependence of these length and time scales on growth parameters is in agreement with dimensional analysis and numerical simulations [7].

Our approach also predicts the presence of a nonlinear term of the form $\Delta(\nabla h)^2$ on large scales, which was suggested previously on heuristic grounds [9, 10]. By power counting it is seen to be relevant in the long time limit and it has nontrivial effects on the scaling behavior [25].

Two extensions of this work seem to be possible within the conserved Sine–Gordon ansatz: First, renormalization of a tilted surface (as performed for the original Sine–Gordon model in Ref.[14]) should clarify the influence of a small miscut on the damping of growth oscillations [2]. Second, and more ambitiously, the implementation of an Ehrlich–Schwoebel–effect [4] may provide a systematic approach to computing the surface current induced by step edge barriers [9, 11, 26], and thus contribute to understanding the transition from layer-by-layer growth to a coarsening mound morphology [11, 27].

Acknowledgements: We thank H. Kallabis for helpful discussions. This work was supported by Deutsche Forschungsgemeinschaft within SFB 237 *Unordnung und grosse Fluktuationen*.

A Appendix: Scaling Functions

The functions used in the flow equations (28,i) and (28,ii) are

$$\begin{aligned} g(\mathcal{K}/\kappa,\theta) &= 8\pi^5 \ \frac{1-e^{-2\mathcal{K}\theta/\kappa}}{[(\mathcal{K}/\kappa)^2+\pi^2]^3} \\ &\quad \Big[\mathcal{K}/\kappa\Big(-(\mathcal{K}/\kappa)^4-4\pi^2(\mathcal{K}/\kappa)^2+5\pi^4\Big) \\ &\quad +\Big(B\ \cos(2\pi\theta)+A\ \sin(2\pi\theta)\Big)\ \ e^{-2\mathcal{K}\theta/\kappa}\Big] \\ f(\mathcal{K}/\kappa,\theta) &= 16\pi^6 \ \frac{1-e^{-2\mathcal{K}\theta/\kappa}}{[(\mathcal{K}/\kappa)^2+\pi^2]^3} \\ &\quad \Big[\pi\Big(-(\mathcal{K}/\kappa)^4-8\pi^2(\mathcal{K}/\kappa)^2+\pi^4\Big) \\ &\quad +\Big(-A\ \cos(2\pi\theta)\ \ +B\ \sin(2\pi\theta)\Big)\ \ e^{-2\mathcal{K}\theta/\kappa}\Big] \end{aligned}$$

with the polynomials

$$A \ = \ 4\pi\theta^2(\mathcal{K}/\kappa)^6+(\pi-8\pi^3\theta^2)(\mathcal{K}/\kappa)^4$$

$$
\begin{aligned}
& +8\pi^3\theta(\mathcal{K}/\kappa)^3 + (8\pi^3 - 4\pi^5\theta^2)(\mathcal{K}/\kappa)^2 \\
& +8\pi^5\theta\mathcal{K}/\kappa - \pi^5 \\
B \;=\; & -4\theta^2(\mathcal{K}/\kappa)^7 + 4\theta(\mathcal{K}/\kappa)^6 + (1 - 8\pi^2\theta^2)(\mathcal{K}/\kappa)^5 \\
& +16\pi^2\theta(\mathcal{K}/\kappa)^4 + 4(\pi^2 - \pi^4\theta^2)(\mathcal{K}/\kappa)^3 + 12\pi^4\theta(\mathcal{K}/\kappa)^2 \\
& -5\pi^4\mathcal{K}/\kappa.
\end{aligned}
$$

References

[1] J.M. Van Hove, C.S. Lent, P.R. Pukite and P.I. Cohen, Damped oscillations in reflection high energy electron diffraction during GaAs MBE, *J. Vac. Sci. Technol. B* **1** (1983) 741; P.K. Larsen and P.J. Dobson, eds., "Reflection High-Energy Electron Diffraction and Reflection Imaging of Surfaces", Plenum, New York (1988).

[2] P.I. Cohen, G.S. Petrich, P.R. Pukite, G.J. Whaley and A.S. Arrott, Birth-death models of epitaxy: I. Diffraction oscillations from low index surfaces, *Surf. Sci* **216** (1989) 222; G.S. Petrich, P.R. Pukite, A.M. Wowchak, G.J. Whaley, P.I. Cohen and A.S. Arrott, On the origin of RHEED intensity oscillations, *J. Cryst. Growth* **95** (1989) 23.

[3] R. Kunkel, B. Poelsema, L.K. Verheij and G. Comsa, Reentrant layer-by-layer growth during molecular-beam epitaxy of metal-on-metal substrates, *Phys. Rev. Lett.* **65** (1990) 733; B. Poelsema, A.F. Becker, G. Rosenfeld, R. Kunkel, N. Nagel, L.K. Verheij and G. Comsa, On the shape of the in-phase TEAS oscillations during epitaxial growth of Pt(111), *Surf. Sci.* **272** (1992) 269; T. Michely, M. Hohage, S. Esch and G. Comsa, The effect of surface reconstruction on the growth mode in homoepitaxy, *Surf. Sci.* **349** (1996) L89.

[4] G. Ehrlich and F.G. Hudda, Atomic view of surface self-diffusion: Tungsten on tungsten, *J. Chem. Phys.* **44** (1966) 1039; R.L. Schwoebel and E.J. Shipsey, Step motion on crystal surfaces, *J. Appl. Phys.* **37** (1966) 3682.

[5] J.H. Neave, P.J. Dobson, B.A. Joyce and J. Zhang, Reflection high-energy electron diffraction oscillations from vicinal surfaces - a new approach to surface diffusion measurements, *Appl. Phys. Lett.* **47** (1985) 100.

[6] D.E. Wolf, Computer simulation of molecular beam epitaxy, *in:* "Scale Invariance, Interfaces and Non-Equilibrium Dynamics", M. Droz, A.J. McKane, J. Vannimenus and D.E. Wolf, eds., Plenum Press, New York (1995), p. 215.

[7] H. Kallabis, L. Brendel, J. Krug and D.E. Wolf, Damping of oscillations in layer-by-layer growth, *Int. J. Mod. Phys. B* (in press).

[8] See, for example, J. Villain, A. Pimpinelli and D. Wolf, Layer by layer growth in molecular beam epitaxy, *Comments Cond. Mat. Phys.* **16** (1992) 1, and [6].

[9] J. Villain, Continuum models of crystal growth from atomic beams with and without desorption, *J. Phys. France I* **1** (1991) 19.

[10] Z.-W. Lai and S. Das Sarma, Kinetic growth with surface relaxation: Continuum versus atomistic models, *Phys. Rev. Lett.* **66** (1991) 2348.

[11] J. Krug, Origins of scale invariance in growth processes, *Adv. Phys.* **46** (1997) 139.

[12] W.W. Mullins, Solid surface morphologies governed by capillarity, *in:* "Metal Surfaces: Structure, Energetics and Kinetics", N.A. Gjostein and W.D. Robertson, eds., American Society of Metals, Metals Park (1963).

[13] J. Krug, Continuum equations for step flow growth, *in:* "Dynamics of Fluctuating Interfaces and Related Phenomena", World Scientific, in press.

[14] P. Nozières and F. Gallet, The roughening transition of crystal surfaces. I. Static and dynamic renormalization theory, crystal shape and facet growth, *J. de Physique* **48** (1987) 353.

[15] M. Rost and H. Spohn, Renormalization of the driven sine-Gordon equation in 2+1 dimensions, *Phys. Rev. E* **49** (1994) 3709.

[16] L.-H. Tang and T. Nattermann, Kinetic roughening in molecular beam epitaxy, *Phys. Rev. Lett.* **66** (1991) 2899.

[17] J. Krug, Theoretische Aspekte der Molekularstrahlepitaxie, *in:* "Dynamik und Strukturbildung in kondensierter Materie" (Jülich, 1997).

[18] J. Krug, H.T. Dobbs and S. Majaniemi, Adatom mobility for the solid-on-solid model, *Z. Phys. B* **97** (1995) 282.

[19] P. Politi and J. Villain, Kinetic coefficients in a system far from equilibrium (preprint).

[20] P. Politi and J. Villain, Ehrlich-Schwoebel instability in molecular-beam epitaxy: A minimal model, *Phys. Rev. B* **54** (1996) 5114.

[21] T. Sun, B. Morin, H. Guo and M. Grant, Roughening transition of a driven interface with a conservation law, *in:* "Surface disordering: Growth, roughening and phase transitions", R. Jullien, J. Kertész, P. Meakin and D.E. Wolf, eds., Nova Science, New York (1992) p. 45.

[22] H.C. Kang and J.W. Evans, Scaling analysis of surface roughness and Bragg oscillation decay in models for low-temperature epitaxial growth, *Surf. Sci.* **271** (1992) 321; M.C. Bartelt and J.W. Evans, Transition to multilayer kinetic roughening for Metal(100) homoepitaxy, *Phys. Rev. Lett.* **75** (1995) 4250.

[23] M. Kardar, G. Parisi and Y.C. Zhang, Dynamic scaling of growing interfaces, *Phys. Rev. Lett.* **56** (1986) 889.

[24] W.K. Burton, N. Cabrera and F.C. Frank, The growth of crystals and the equilibrium structure of their surfaces, *Phil. Trans. R. Soc. (London) A* **243** (1951) 299.

[25] H.K. Janssen, On critical exponents and the renormalization of the coupling constant in growth models with surface diffusion, *Phys. Rev. Lett.* **78** (1997) 1082.

[26] J. Krug, M. Plischke and M. Siegert, Surface diffusion currents and the universality classes of growth, *Phys. Rev. Lett.* **70** (1993) 3271.

[27] M. Rost and J. Krug, Coarsening of surface structures in unstable epitaxial growth, *Phys. Rev. E* **55** (1997) 3952.

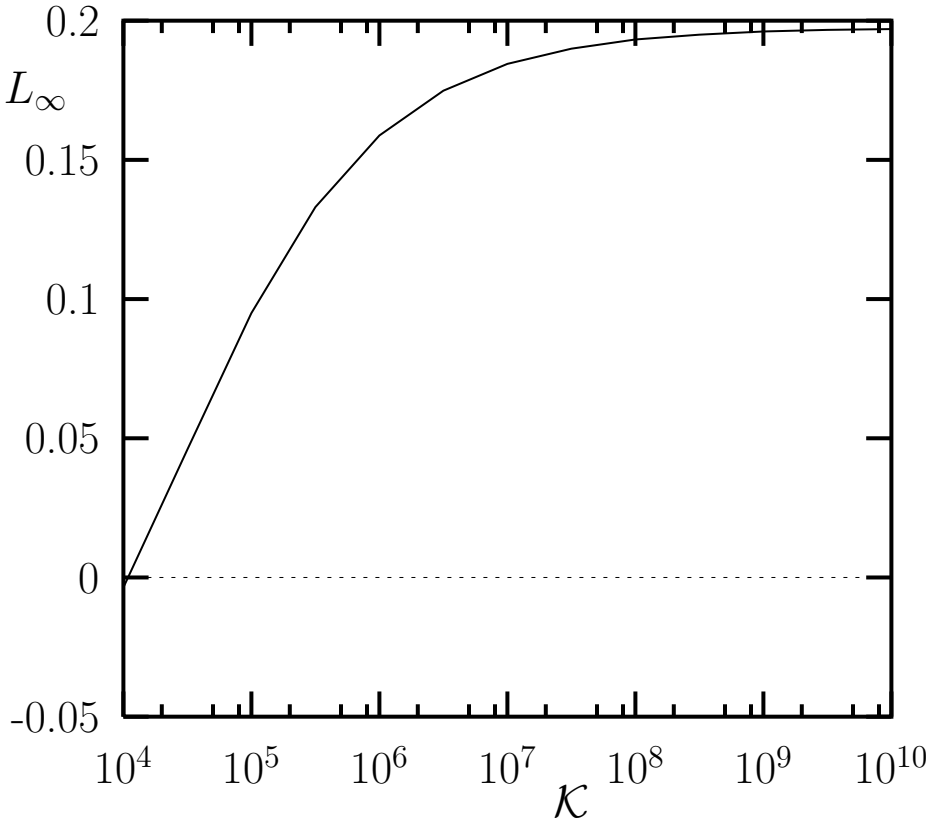

Figure 1
Numerical solution of $L(\kappa \to \infty)$ as defined in Equation (39) using the full flow equations (28). The potential strength is $U_0 = 0.1$; for large values of $\mathcal{K} \geq 10^8$ the value $2\pi^2 U_0^2$ (40) is attained.